The ‘use-by date’ for lithium-ion battery components

Gorman, Scott; Pathan, Tanveerkhan; Kendrick, Emma

DOI:
10.1098/rsta.2018.0299

Document Version
Peer reviewed version

Citation for published version (Harvard):
Gorman, S, Pathan, T & Kendrick, E 2019, 'The ‘use-by date’ for lithium-ion battery components', *Royal Society of London. Philosophical Transactions A. Mathematical, Physical and Engineering Sciences* , vol. 377, no. 2152, 20180299. https://doi.org/10.1098/rsta.2018.0299

PHILOSOPHICAL TRANSACTIONS A

Phil. Trans. R. Soc. A.
doi:10.1098/not yet assigned

The 'use-by date' for lithium-ion battery components

Scott F. Gorman[1], Tanveerkhan S. Pathan[1], Emma Kendrick[1,2*]

[1]*WMG, The University of Warwick, Coventry. CV4 7AL. U.K.*
[2]*School of Metallurgy and Materials, University of Birmingham, Edgbaston, Birmingham. B15 2TT. U.K.*

Keywords: Lithium-ion batteries, Shelf life, electrode degradation, electrode storage

Abstract

Lithium-ion battery (LIB) manufacturing is based around the slurry tape casting of electrodes followed by the assembly of the dried electrodes into cells with a separator and electrolyte. Many aspects of the manufacturing process can affect the performance of a lithium-ion cell. One of the least understood aspects in academia is the effect of degradation of the materials during the manufacturing processes or the 'shelf-life' of the materials and components. Here we discuss some of the time limitations and degradation issues observed during the manufacturing and testing of the components from an industrially sourced $LiNi_{0.6}Mn_{0.2}Co_{0.2}O_2$ (NMC-622)//Graphite cell, and the affect that the component storage has, upon both the performance and the properties of the materials and cells. The materials are stored either in a dry room, vacuum oven or in a laboratory environment and the effect of the atmosphere upon the degradation components of the electrodes and electrolyte is characterised by analytical surface techniques and electrochemical analysis. We note that all storage affects the electrochemical performance, even storage in a vacuum oven or dry room. We propose that the electrodes and electrolytes should be used immediately after manufacture, however we propose alternative methods for storage in case this is not possible.

1. Introduction

LIBs were introduced to the masses in 1990 by Sony(1). Although the manufacturing processes are very similar to those used at the time of their introduction, the tolerances and control of the materials handling during manufacturing has improved and consequently the performances of the cells have improved(2). One aspect of manufacturing that needs to be considered is the storage and handling time for the components during manufacture, the tight controls required adds logistical issues to the supply and storage of materials and can add additional costs with increased scrap rates if not correct(3). The materials degrade during storage however the 'use-by date' of the components is not fully understood. The point at which the electrodes become unusable is a fine balance, and the exposure to air both in a dry room and in atmospheric conditions can affect the lifetime and performance of a cell quite dramatically(4). Residual moisture in the electrodes after manufacturing also reduces the lifetime and performance of the electrodes(5). Therefore, care must be taken to dry the materials completely before use. Temperatures as high as 120 °C are recommended to remove the residual traces of N-Methyl-2-Pyrrolidone (NMP) and water. The absorption of carbonates and water onto the surface of the materials can produce an alkalinity, as has been shown for

*Author for correspondence (e.kendrick@bham.ac.uk).
†Present address: School of Metallurgy and Materials,
University of Birmingham, Edgbaston, Birmingham. B15 2TT. U.K.

$LiNi_{0.8}Mn_{0.1}Co_{0.1}O_2$ (NMC-811) powder(6) and other layered oxide materials(7). This can lead to difficulty in producing stable inks for electrode coatings(8). The alkalinity in an NMP- Polyvinylidene fluoride (PVDF) ink, water content and heat from mixing, causes an instability and the ink gels over time(9). This issue is becoming more prevalent with the adoption of new technologies such as sodium-ion batteries(10). One method of overcoming small levels of alkalinity is by adding an acid into the formulation, which of course produces water as a by-product and may degrade the material before coating(11). The typical non-aqueous electrolytes used are also prone to absorbing moisture from their surroundings and as result, water as a contaminant has deleterious effects on both the electrode and electrolyte performance and their longevity. It has been reported that even at concentrations as low as ~10 ppm, water in the electrolyte can start to promote undesirable side reactions(12). Commercially available electrolytes are typically quoted as having less than 10 ppm water content, however this level is known to increase with time, even when stored under conditions such as a dry room or an argon filled glovebox(13).

In this work, we have investigated NMC-622 cathodes and graphite anodes from an automotive cell. The precise composition of the electrodes with respect to the carbon additives and the binder is unknown. However, the binder for the NMC is likely to be PVDF, and for the graphite; carboxymethyl cellulose - styrene-butadiene rubber (CMC-SBR). The cathode material can be removed from the aluminium current collector with NMP, and the graphite with water. The use of electrodes and the electrolyte during the manufacturing process is strictly time controlled to ensure the quality of the materials used for assembling the cell, and ultimately the cell performance. The shelf life of each material is different; however, from conversations with industry, electrolytes are typically used within a 6-10 week period of manufacture and the electrodes are sealed in evacuated arrangements and then utilised within 2-4 weeks of their opening. This is because the degradation of the materials can have a huge impact upon the lifetime and performance of the cell, the wastage incurred and the consistency of the products(5). In laboratories and research environments length of storage and conditions are also important but more difficult to control.

2. Formation degradation and storage of electrodes

The testing and characterisation in an academic environment should also take into consideration these life-time issues, and we have studied the affect upon the performance properties and the morphological effects upon the electrodes with the different environments in which materials are stored; a dry room, a vacuum oven and in standard laboratory atmosphere.

3. Experimental

In order to study the electrode degradation of a commercial graphite anode and NMC-622 cathode single sided electrodes were made from the received double-sided electrodes by cleaning one side using NMP for the cathode and water for the anode. The electrodes were then dried at in a vacuum oven to remove any residual solvent. The resulting single sided electrodes were then utilised in a range of stability tests in different environments. Three environments were chosen; the dry room (-45° C dew point 8 am-5 pm and -25° C dew point over night), a vacuum oven at 50° C and a laboratory thermostatically maintained at 25° C. The materials were analysed every two weeks over a three-month period by scanning electron microscopy (SEM) and X-ray diffraction (XRD). X-ray photoelectron spectroscopy (XPS) and electrochemical cycling were also undertaken to assess the change in the surface properties of the materials and their affect upon the performance.

The XPS data was obtained using a Kratos Axis Ultra DLD spectrometer. The cleaned, single-sided electrode samples investigated in this study were attached to an electrically conductive carbon tape, mounted on to a copper stub and loaded via an inert atmosphere transfer unit to minimise any change in the electrode surface from reaction with air; especially in case of samples from dry room and vacuum oven. XPS measurements were performed at room temperature using a monochromated Al kα X-ray source and at a take-off angle of 90° with respect to the surface parallel. The core level spectra were recorded using a pass energy of 20 eV

(resolution approx. 0.4 eV), from an analysis area of 300 μm x 700 μm. The spectrometer work function and binding energy scale were calibrated using the Fermi edge and 3d {5/2} peak recorded from a polycrystalline Ag sample prior to the commencement of the experiments. Due to the insulating nature of the samples, charge neutralisation of the surface was required and necessitated recalibration of the binding energy scale. To achieve this, the main C-C/C-H component of the C 1s spectrum, corresponding to adventitious carbon, was referenced to 284.3 eV. The data were analysed with the CasaXPS software package, using Shirley backgrounds and mixed Gaussian-Lorentzian (Voigt) line shapes and asymmetry parameters where appropriate. For compositional analysis, the analyser transmission function has been determined using clean metallic foils to determine the detection efficiency across the full binding energy range.

XRD measurements were taken on a PANalytical Empyrean using a cobalt X-ray source (not monochromated) and a PANalytical X-pert detector. Scans were run from 15° to 85° 2θ over a period of 45 minutes, with a step size of 0.013°. Samples were mounted on a standard powder diffraction sample holder, with the indent filled to present the electrode at the top of the indent to reduce any zero-point errors. The baseline samples were analysed using High Score in order to get a phase ID.

SEM images were acquired using a Thermo Scientific™ FEI SCIOS™ Dual Beam™ which is an ultra-high-resolution dual beam system. An SE R580 detector was used to detect secondary electrons. An Oxford Instruments X-Max 150 EDS system was used to undertake Energy-dispersive X-ray spectroscopy (EDS) analysis with an Oxford Instruments INCA software for SEM. The working distance was maintained between 7.0 mm and 7.5 mm with an aim to be closer to 7.0 mm. Images have been obtained using secondary electrons (SE), backscattered electrons (BSE) and an in-lens detector which also looks at conventional SE from above the sample surface. In all cases, the accelerating voltage was 3 keV (except for fresh samples where the accelerating voltage was 5 keV) and the probe current was 0.4 nA for all samples. When undertaking compositional analysis using EDS, the accelerating voltage was ramped up to 10 keV in order to capture sufficient electrons to generate the elemental peaks.

Half-cells *vs.* lithium metal were built from the stored electrodes utilising CR2032 coin cell casings (Hohsen Corp., Japan) Figure 1. The electrodes were comprised of a 15.0 mm diameter discs of lithium and 14.8 mm diameter discs of the cleaned single-sided storage samples. A standard tri-layer separator was used (polypropylene – polyethylene – polypropylene, Celgard® 2325 – 1850M – BM68) with a PuriEL Battery Electrolyte from soulbrain (Michigan, USA). The electrolyte composition was 1.0 M lithium hexafluorophosphate ($LiPF_6$) in a mixed solvent of propylene carbonate (PC): ethylene carbonate (EC): diethyl carbonate (DEC) (1:1:3 by volume). Each coin cell was filled with an excess of electrolyte (60 μL). A stainless steel (316L) spacer and wave string are also housed inside the casing to ensure uniform compression through the layers. The cells were then tested using Bio-Logic BCS 805 series cyclers using the following protocol: first charge and discharge at C/10 using CC/CV/CC (constant current charge, constant voltage at the upper voltage till the current drops to 10% of the original applied current and constant current discharge). The cells were charged up to 4.2 V for cathodes, with a subsequent electrochemical impedance spectroscopy (EIS) scan. The frequency range used was 10 kHz to 100 mHz, with a 10 mV perturbation voltage. Cells were held at the desired potential for 30 min prior to making EIS measurements. The cells were held at open circuit potential for 14 days, and then a second EIS measurement taken before cycling for 50 cycles at C/2 with CC/CV/CC, between the voltage limits 3 V and 4.2 V *vs.* Li metal for cathode. In case of the anode half cells, the cells did not cycle to generate enough data for comparative analysis.

Full cells were made with the single-sided anode and cathode at a ratio of 2.2 mAh cm^{-2} to 2.0 mAh cm^{-2}. Two sets of three cells each were made; one for as-received electrodes and one for the electrodes stored in a vacuum oven for 5 month. Two slow charge /discharge formation cycles at C/20 were run for forming the cells using CC/CV/CC protocol between 4.2V and 2.5V. The cells were then cycled at C/2 with CC/CV/CC

protocol between 4.2V and 2.5V. EIS scans were obtained from the two sets of cells over the period of the cycle life; immediately after formation, after 50, 100, 200 and 500 cycles.

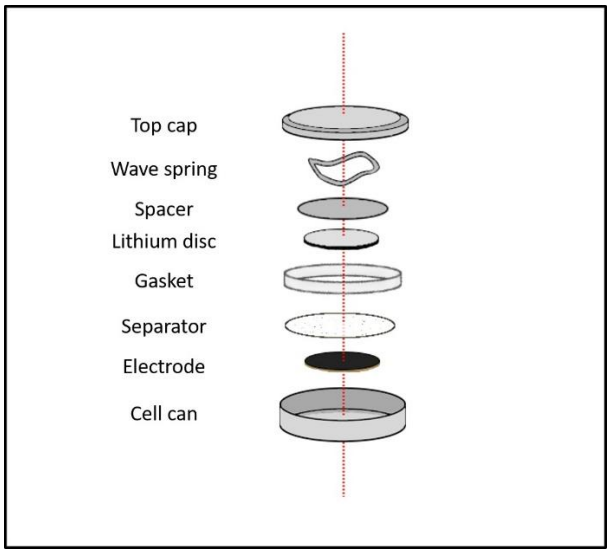

Figure 1: Exploded diagram illustrating the assembly of half-cell coin cell prior to electrochemical testing

4. Results

4.1. Surface Analysis: Anode and Cathode

a. Cathode

Samples cut from the NMC cathodes stored in the three environmental conditions, vacuum oven, dry room and standard laboratory conditions were evaluated initially at two-week intervals and then every 4 weeks once it became apparent that variation was minor. There was not an overriding obvious change in the position of the X-ray patterns indicating negligible lithium removal from the structure. A secondary peak appeared at low angles (approx. 16° 2θ) after 4 weeks, which was assigned to hydrated layered oxide material. This additional peak was observed in all the samples after 4 weeks and it persisted for the remainder of the storage trial. A representative XRD is shown in Figure 2, the expansion highlights the emergence of the new peak, which could be due to the c axis expansion of the crystal lattice with water incorporation.

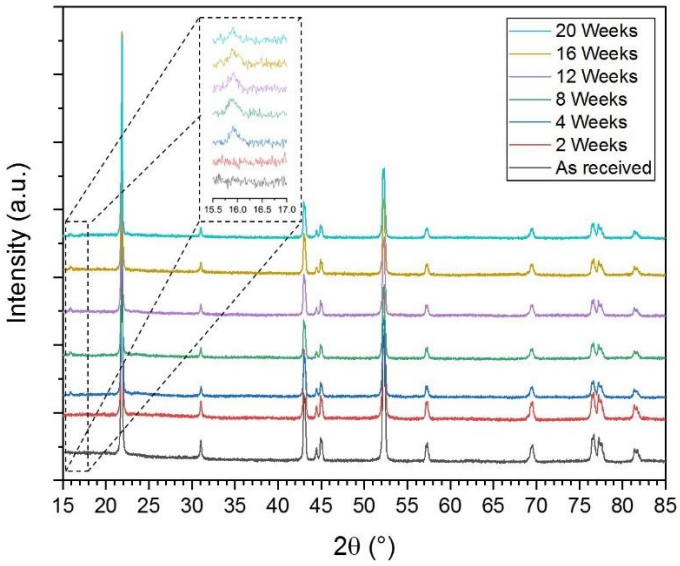

Figure 2: X-ray diffraction patterns for the NMC based cathode acquired at 2-4 week intervals stored in a dry room. Minimal variation is discernible except for the appearance of a secondary peak (~16° 2θ) at 4 weeks assigned to hydrated layered oxide materials

The surfaces of the as-received 'fresh' electrodes and the electrodes stored under the three environmental conditions have been analysed using SEM to study the effect of storage conditions on electrode surface morphology. Samples taken from each of the storage environments were imaged at approximately 3-week intervals.

SEM images revealed that the cathode comprised of primary particles of approximately 1 μm which are aggregated forming larger particulates of broad particle size distribution ranging from a few microns to up to 25-30 μm in diameter (Figure 3). The cathodes stored under laboratory conditions showed some signs of surface cracks however, the samples stored in the other two environments, the vacuum oven and dry room, did not appear to visually alter during the period of storage (Figure 4). There is large variation in the surface roughness within individual samples. Certain regions appear to be flat whereas others have crevasses and undulations. The flat areas likely represent portions of the surface, which were in relief prior to calendaring and have subsequently been compressed. It is therefore non-trivial to compare like for like regions due to the initial irregularity of the surface. EDS analysis confirmed the presence of the transition metals on the cathodes with some carbon-based additives (Figure 5 and Figure 6).

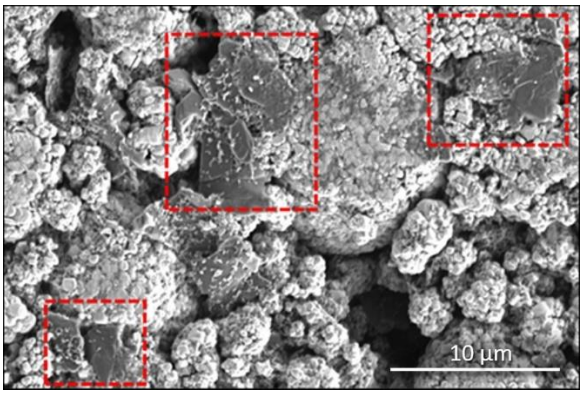

Figure 3: SEM image of cathode surface at 6000x magnification, showing the active material forming clusters of smaller primary articles. The red dotted boxes highlight particles of a carbon-based additive on the cathode surface

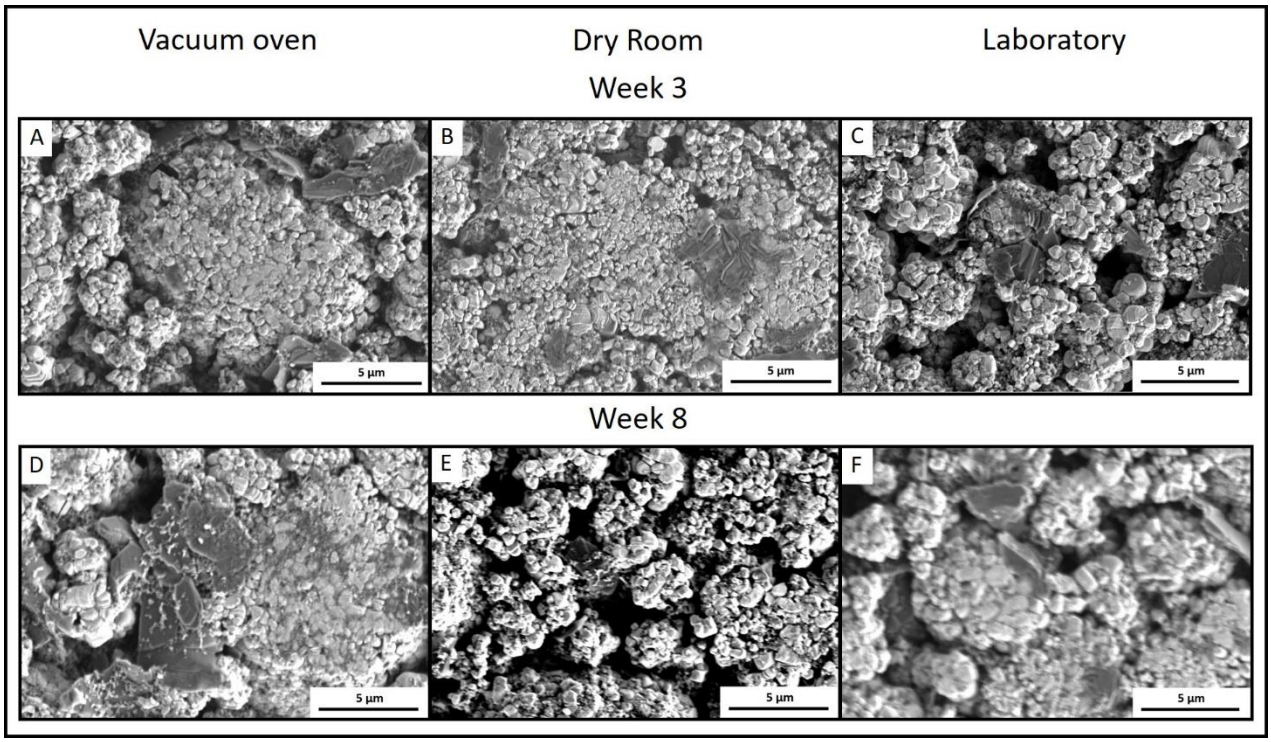

Figure 4: A comparison of SEM images acquired for cathode samples under the different storage conditions as-received, at 3 weeks and after 8 weeks. Surfaces changes as a function of time and storage conditions are slight and there is large variation in the surface roughness within individual samples

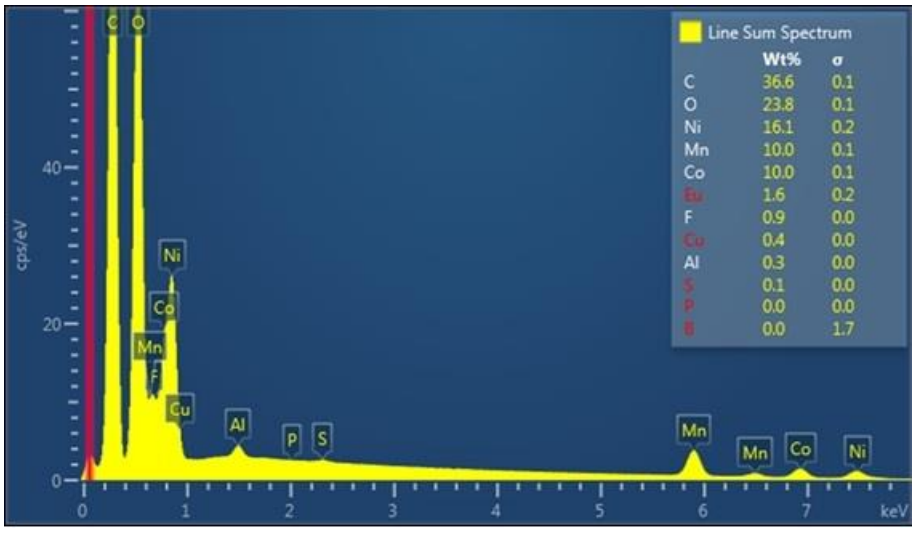

Figure 5: EDS data showing the approximate elemental composition of the cathode

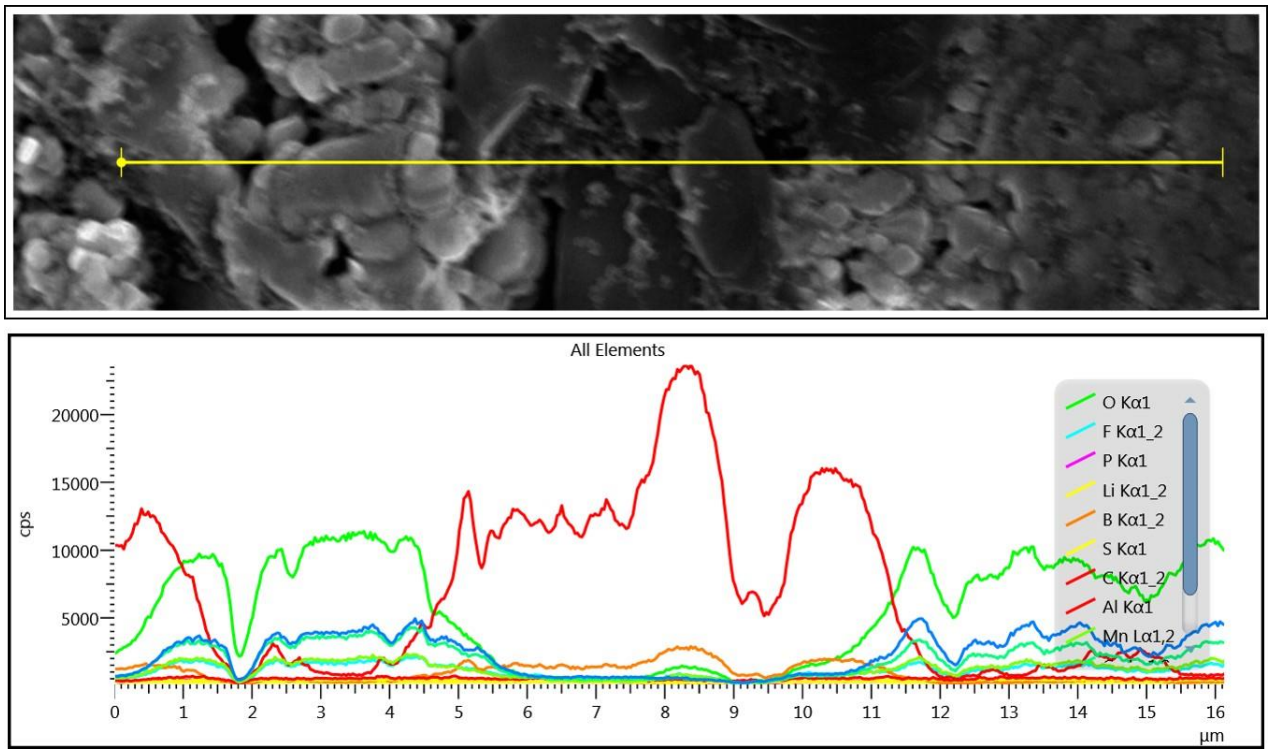

Figure 6: An EDS line scan showing the approximate elemental composition of the cathode along the line

In addition, to the SEM analysis, the surface of the as-received 'fresh' electrodes and the electrodes stored under the three environmental conditions have been analysed using XPS to study the effect of storage conditions on the surface composition of the electrodes. XPS analysis was conducted at week 12. Peak positions as well as the calculated percentages for the different constituent components for the identified peaks are displayed in Table 1**Error! Reference source not found.** and the change in the oxygen species with different storage conditions in Figure 7.

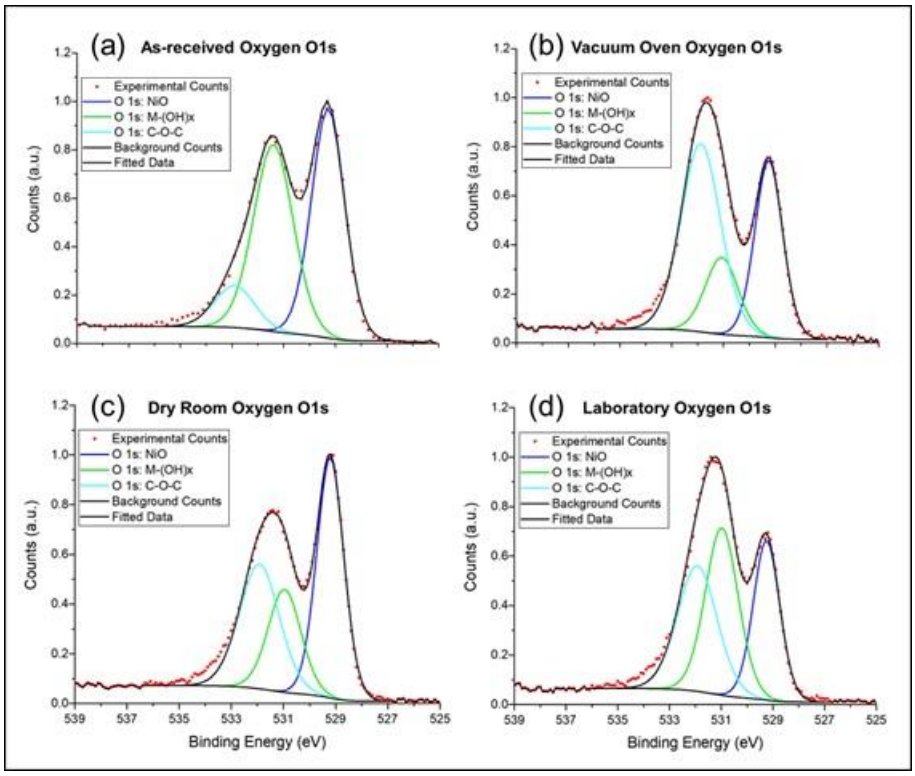

Figure 7: XPS data for the Oxygen 1s peaks observed for cathode samples a) as received 'fresh', b) stored in a vacuum oven, c) stored in a dry room, d) lab

The XPS analysis reveals a clear difference in the surface composition of the as-received cathodes and the cathodes stored under the three different environments for a period of 9 weeks. The elemental composition of all four cathodes is listed in Table 1. In case of all four samples, the oxygen (O1s) peaks consisted of nickel oxide (binding energy around ~529.2), transition metal hydroxides (~530.9) and C-O-C bonds (~531.9). For the as-received cathode, oxygen made up to around 20% of the overall surface analysed. This is reduced to ~13.5% for the vac oven samples and ~18.7% for the dry room samples. Figure 8 shows the effect of oxygen and moisture on the elemental composition of the samples. As discussed, the vac oven samples had a reduced amount of oxygen as compared to the dry room samples and both of them being lower than the as-received samples. This can be attributed to the temperature and vacuum conditions inside the oven and the lack of any more oxygen or moisture. The dry room samples show a similar trend; however, they have slightly more oxygen which is available in the atmosphere. The laboratory samples resulted in an increased amount of oxygen which would be readily available in the atmosphere they were stored in. Within the oxygen bonding environment for the as-received samples, nickel oxide and the metal hydroxides (14,15) made up to ~45% each and 10% being C-O-C. The metal hydroxides are reduced to ~17% for the vac oven samples showing the effect of vacuum environment. The metal hydroxides still make up large proportion of oxygen in the laboratory samples as seen in Figure 7. The effect of moisture is seen with increased hydroxide proportion in laboratory samples compared to the dry room and vacuum oven samples. As the materials are aged in the different environments the levels of graphitic carbon on the surface decrease (from the conductive additive), and the proportions of transition metal and lithium oxides increase. This is likely due to the hydroxide and carbonate species on the surface, and a slight expansion of the cathode particles as a result and the obscuring of the conductive additive species.

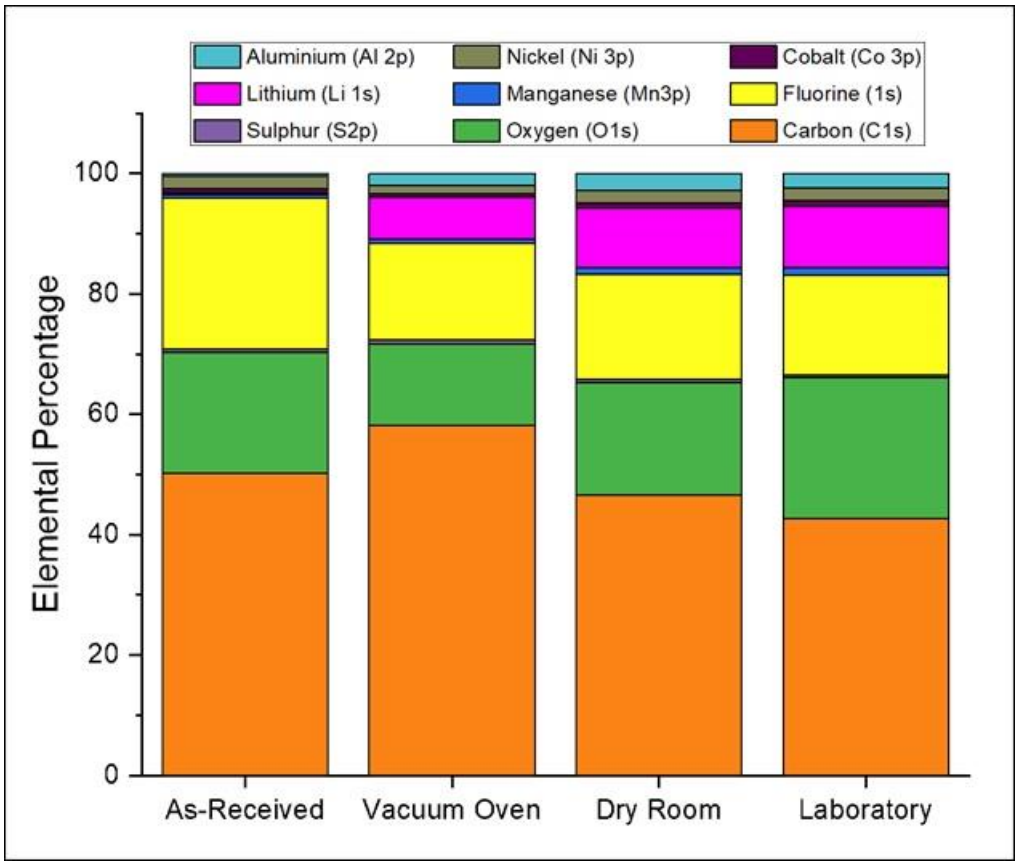

Figure 8: The proportion of surface elements after cathode electrode storage in different environments for 12 weeks

b. Anode

X-ray diffraction was performed on the graphite anode electrode, after exposure to the different environments every two weeks. The material was predominantly graphite, additional peaks in the spectra were observed representing a carbon additive. No shift in peak position was observed in the X-ray patterns was observed as a function of time for any of the storage conditions. Therefore, based on X-ray diffraction the anode was not observed to change structure over time. A representative X-ray pattern is shown in

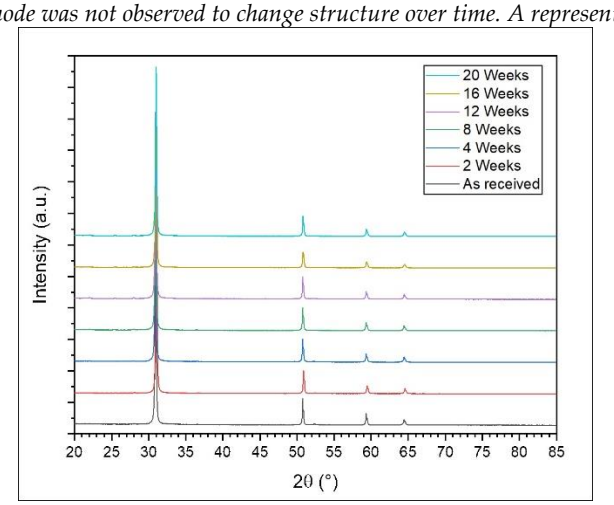

Figure 9.

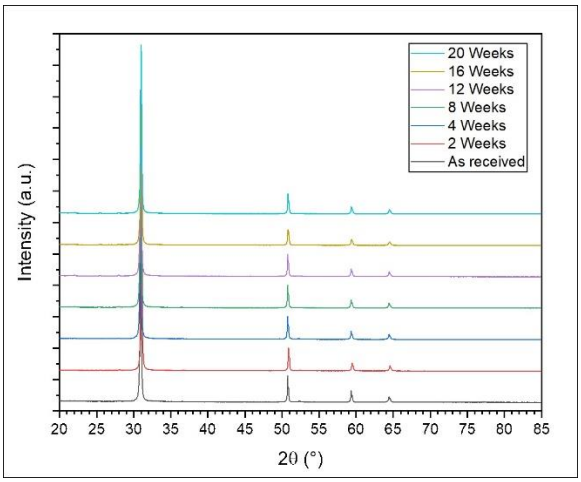

Figure 9: X-ray diffraction patterns for the carbon-based anode, stored in a dry room, acquired at 2-4 week intervals showing minimal variation in peak position over a three month period

SEM images of the as-received anode reveal ellipsoid 'bolder-like' graphitic particles with a diameter of approx. 15-25 μm (Figure 10). The general observation was that in the case of the vacuum oven, the anodes maintained their structure for the duration of storage whereas those in standard atmosphere developed fissures on the surface of the anode. The dry room samples also displayed some signs of surface cracking after 8 weeks of storage (Figure 11). There is a trend therefore for an increased propensity to form these fissures, or particle pulverisation, more rapidly the 'wetter' the storage condition. The fact that the surface morphology has been physically altered also suggests that the process is irreversible and so a heat treatment prior to cell assembly may not restore the electrodes original properties, although is not reported here in this study.

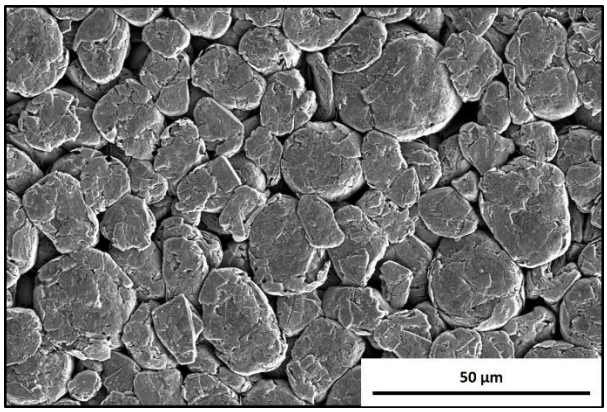

Figure 10: SEM image of the as-received anode at x1,500 magnification obtained using the secondary electron detector. The graphitic particles are 'bolder-like' in form with smooth unbroken surfaces

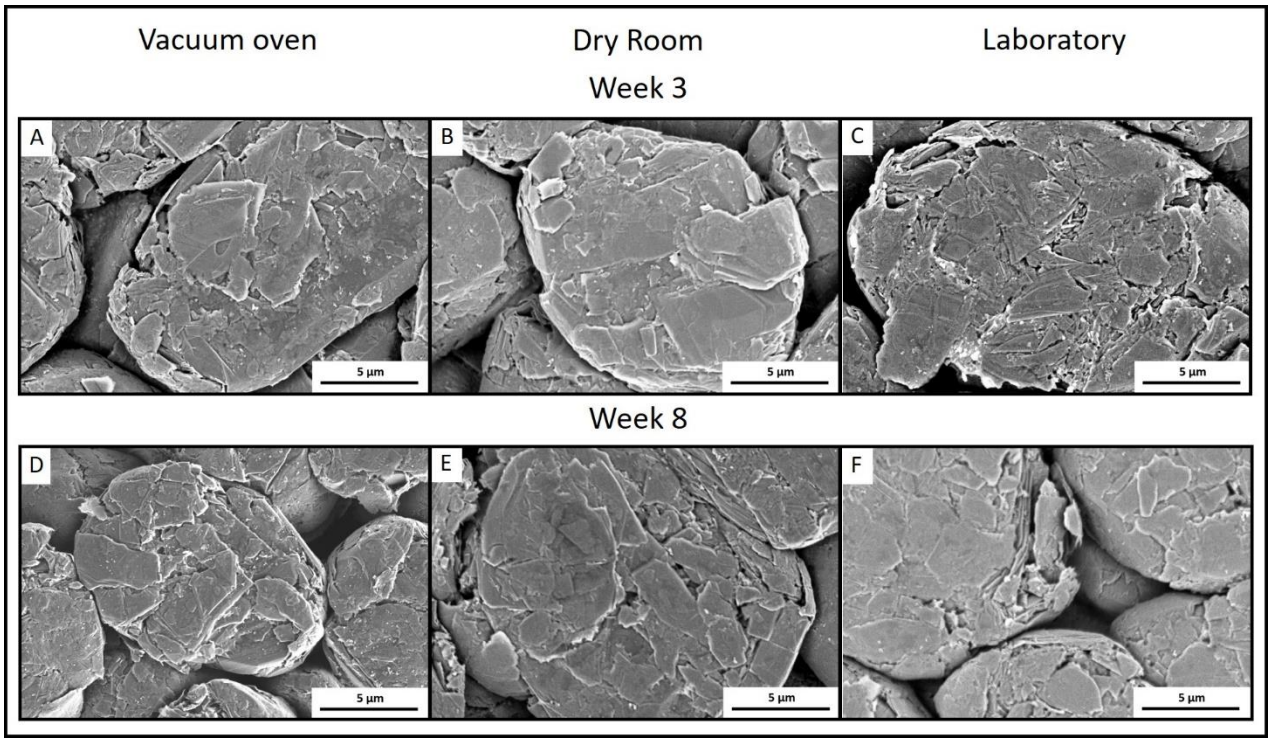

Figure 11: A comparison of SEM images acquired for anode samples under the different storage conditions as-received, after 3 weeks and after 8 weeks. There are visible fissures on the samples stored under 'wetter' conditions

Similar to the cathode XPS analysis, the 'as received' electrodes as well as samples from the different storage environments were analysed after 9 week of storage for the anodes. These mostly comprise of carbon from the graphite that makes up most of the anode surface. The peak positions as well as the calculated percentages for the different constituent components for the identified peaks are displayed in Table 2 which shows that the oxygen content is lower in the vacuum oven (~14.4%) as compared to the dry room (~15.5%) or the laboratory (~15.9%). These results indicate more absorbed species in the samples stored in air. The proportion of the surface species are very similar between the different storage conditions. XPS is a surface technique and if the absorbed species are penetrating the particles causing low levels of exfoliation, as is indicated from the SEM images, this technique may not pick up this nuance. The SEM and XPS results suggest that storage in a vacuum oven is preferential however; it does not entirely mitigate degradation of the electrode. The limited change in the oxygen content with different storage conditions is shown in Figure 12.

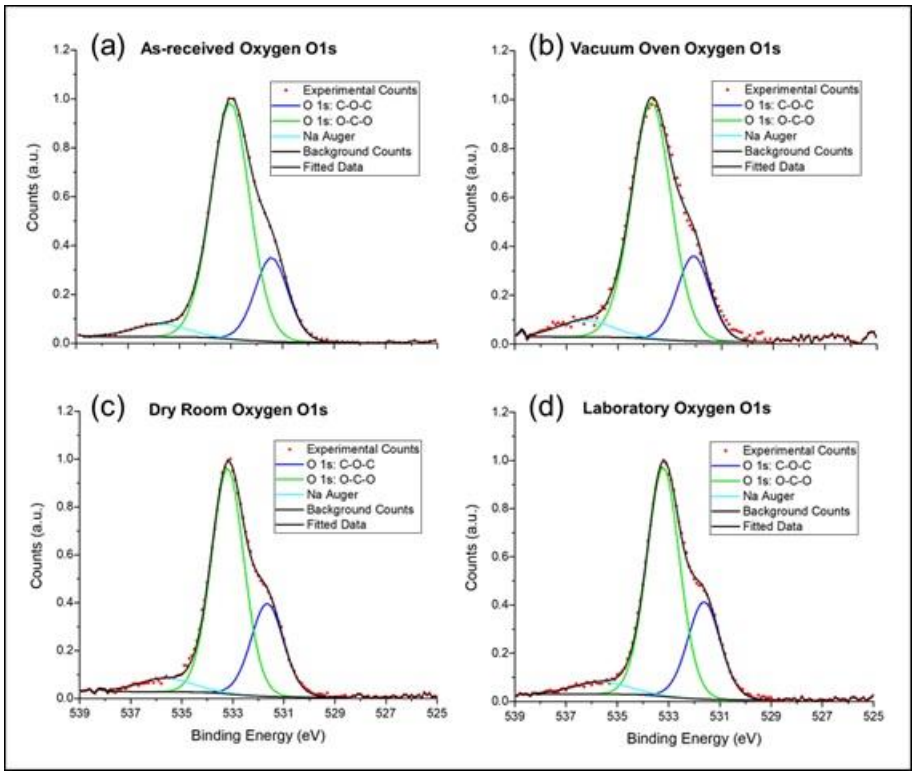

Figure 12: XPS data for the Oxygen 1s peaks observed for anode samples a) as received 'fresh', b) stored in a vacuum oven, c) stored in a dry room, d) lab

4.2. Half Cell Formation and Cycling

Cathode half-cells vs. a metallic lithium disk as a counter/reference electrode were built concurrently to the X-ray diffraction measurements. The cells were charged to 4.2 V vs. Li and cycled between 4.2 V and 3.0 V vs. Li to investigate their specific capacity fade after storage in the different environments. As discussed earlier, the anode half cells did not cycle to generate comparative data. The first and second cycle information showing the observed specific capacities and the voltage drop during the ageing period are shown in

Table 3. Although at first glance there is not much of a difference between the aged electrodes, the 1st cycle loss increases from 12 to 16% during the 2 to 20 week exposure period, whereas the dry room loss remained at 12% and the standard laboratory sample around 11%. The main observation is the reduction in the formation capacity and the discharge capacity for the electrodes stored in the dry room and at standard room temperature and humidity, 0.18 mA h to 0.135 mA h and 0.16 mA h to 0.133 mA h for the two storage conditions respectively. For the materials stored in the vacuum chamber this is not the case and although there is drop in discharge capacity (0.09 mA h) there is no observable trend in the formation capacities. In all cases, the formation capacity is greater for the electrodes stored in the vacuum oven compared to the dry room or general atmosphere.

Storage in the dry room has quite a significant effect on the quality of the electrodes, both anode and cathode. When stored in a vacuum oven there is no observable major change in the initial capacities of the anodes, there is a small increase in the first cycle loss. However, there is a significant change in the surface properties, possibly due to the de-absorption of carbon dioxide species. The cathodes show a decrease in formation

capacity and an associated increase in the surface carbonates and hydroxides on the surface of the materials. In case of cathodes, there is an observed increase in the level of lithium and oxygen on the surface, compared to the as received materials and for the severely exposed materials, increased cracking of the particles was observed, this results in a loss of electronic connectivity of the electrodes; which is the likely reason for the reduced capacity of the electrodes.

4.3. Full Cell Analysis

The resistance originating from the secondary electrolyte interphase (SEI) layer is tracked (*Figure 13* and *Figure 14*). The first incomplete semi-circle in the high to medium frequency range is the resistance arising from the charge transfer between the electrolyte and the solid surfaces. The second semicircles (*Figure 13* and *Figure 14*) in the medium to low frequency range results from the lithium ion migration from the surface films. The linear Warburg element at the low frequency range corresponds to the lithium ion diffusion through the active material. For simplicity, only the SEI resistance arising from the diffusion of lithium ion through the surface films is taken into calculations. It is observed that the impedance on the vacuum stored sample is slightly lower than the pristine sample after the formation, however the impedance increases significantly from ~10 ohms to ~50 ohms over the 500 cycles. It also shows the large increase in impedance after 100 cycles which corresponds to the cycle life fade shown in Figure 15; whereas the pristine sample resistance increases from ~14 ohms to ~18 ohms (Table 4). Full cells manufactured using electrodes cut from the same batches of coatings months' apart show a significant disparity in cycle life. Figure 15 shows averaged cell capacity vs. cycle life for three cells made with as-received electrodes and three made using electrodes stored in a vacuum oven for 5 months. Although initial capacity is similar for cells produced immediately after electrode production and after 5 months of storage the capacity as a function of cycle life, began to diverge rapidly. After only 100 cycles the capacity of the electrodes stored in the vacuum chamber drops off a 'cliff' whereas the fresh sample maintains a steady discharge capacity degrading in a more gradual manner. This illustrates the stark comparison between cells produced using 'fresh' electrodes and those, which have experienced degradation as a result of storage even in a vacuum oven.

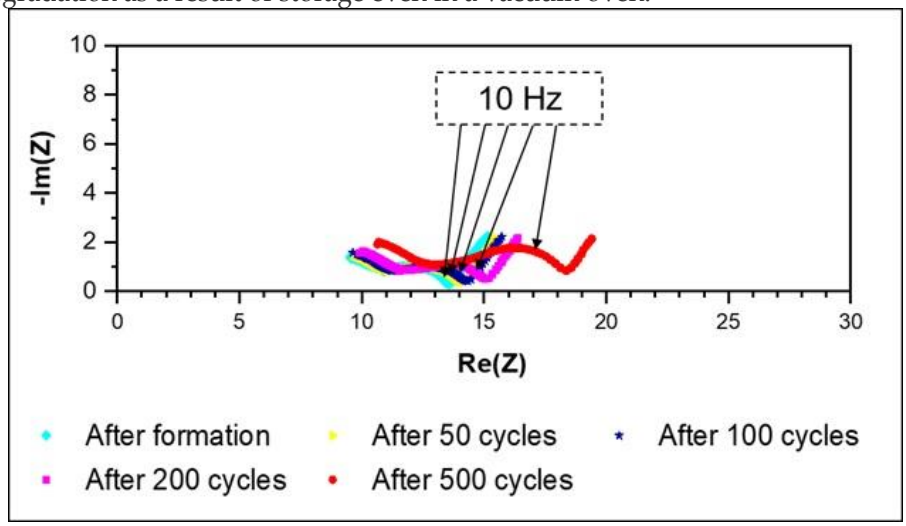

Figure 13: Impedance data for full cells made from 'fresh' electrode samples at 25 °C recorded at various stages during the formation and cycling protocol, showing the appearance of a second semicircle after formation of the SEI and consistent r values

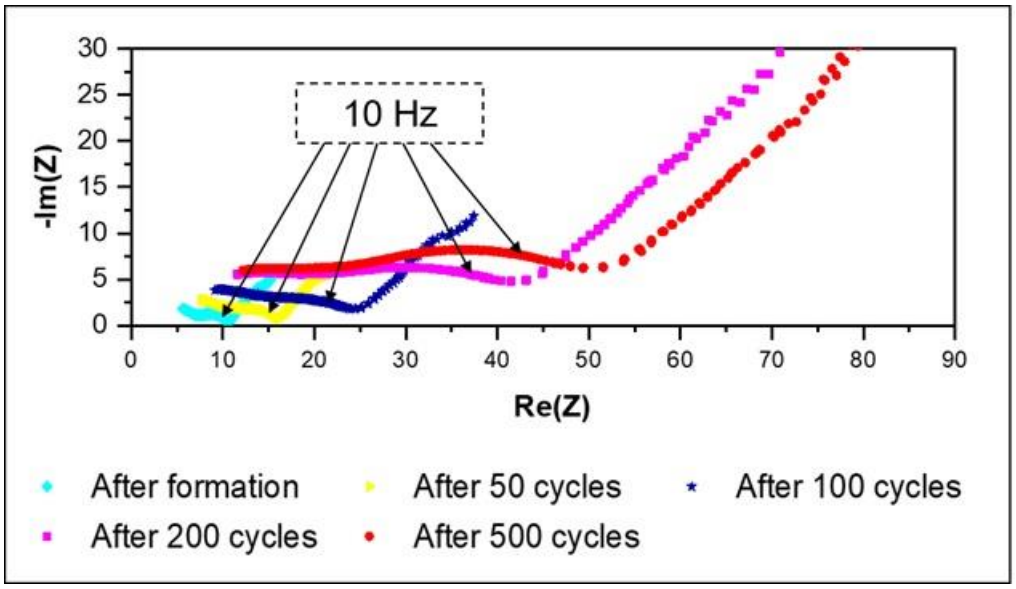

Figure 14: Impedance data for full cells made using electrodes stored for 5 months in a vacuum oven recorded at various stages during the formation and cycling protocol, showing significant increase in resistance values with cycling compared to the cells shown in Figure 13

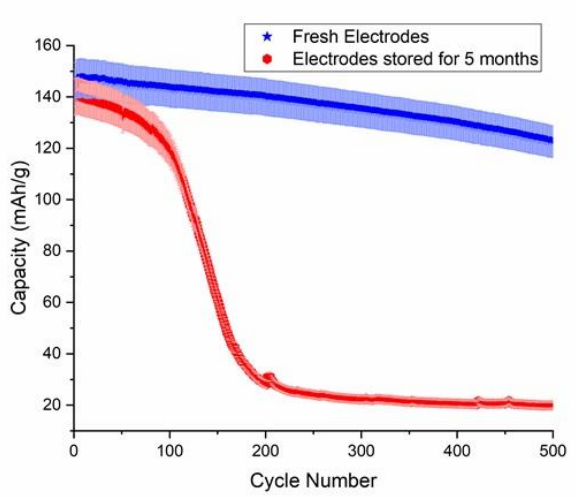

Figure 15: Cell capacity vs. cycle life plot for cells assembled using fresh electrodes and electrodes stored under vacuum for 5 months

4.4. Electrolyte

Electrolyte degradation is also of critical importance. It was observed that dependent on the additives incorporated electrolyte was sensitive to both temperature and moisture exposure. For some electrolyte compositions there was a dramatic colour change from clear to orange-brown which occurred in only a few days Figure 16. There is also a dramatic change to the pH of a solution as a result of the production of HF and its derivatives due to parasitic side reactions between the lithium salt and moisture. The concentration of HF produced was far greater than anticipated and led to noticeable etching of glass sample holders and a pH change from approx. 6.5 for as-received samples down to < 1 after the electrolyte had been exposed to air for even short periods (Figure 17). HDPE containers were used for visual purposes however degradation was also witnessed with stainless steel bottles more commonly used commercially. HF production and the

associated acidification of the electrolyte occurred even with limited exposure to a dry room environment and so further investigation is under way to establish best practice for electrolyte storage and handling.

Figure 16: Image to demonstrate the change in colour from clear to orange-brown of electrolyte samples with different additives after 12 days of storage

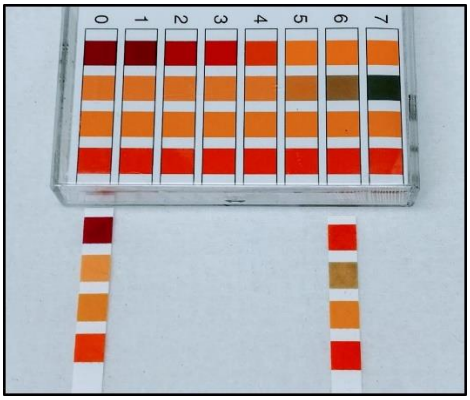

Figure 17: Image to demonstrate the change in pH between RHS) a 'fresh' as-received electrolyte sample approx. 10 ppm water and LHS) an aged sample regularly handled and stored in a dry room

5. Conclusions

The understanding of the shelf-life issues of lithium-ion battery components are critically important as they have a significant impact upon the life-time and performance of a lithium-ion cell. Here we look at components, specifically the electrodes and electrolyte. We have shown that both electrodes, anode and cathode change over time, the storage of the materials in normal atmosphere has enhanced degradation as expected compared to that stored in a dry room and a vacuum oven. However, the degradation even in a vacuum oven can be significant and the demonstration of cells made with the same electrode that cycle only 100 cycles and reach 80% of initial capacity compared to 500 cycles or more with the pristine electrodes illustrates this extremely well. Electrolyte storage and handling is also associated with a shelf life, and in this study, we can see that the degradation of the electrolyte happens even in a dry room. Typically, there is a 6-month shelf life on the electrolyte from the manufacturers; however, this will change depending upon the storage conditions. Water is the biggest culprit for the electrolyte causing decomposition reactions to HF in the electrolyte. Carbon dioxide and water is an issue for electrodes as the surface of the materials absorb CO_2, which eventually hydrolyses to incorporate water and to form lithium hydroxide on the surfaces. In summary the handling, and control of the atmosphere during cell assembly and manufacture is extremely important. Storage in a dry room, and even a vacuum oven in a dry room can have a significant impact upon the cell performances. Although conditions are 'dry' degradation still occurs, and care must still be taken

when using electrodes stored in a vacuum oven. From this work it is very difficult to make a call upon the length of time an electrode should be stored, as all storage has an impact upon the performance, however we would recommend not storing the electrodes under a dynamic vacuum as this appears to also cause degradation issues, the precise mechanisms and the effect of the different binders requires more investigation. We recommend that the electrodes are vacuum-sealed after manufacture and drying and subsequently only opened within the same week of use. Electrolyte should be stored in inert atmospheres and only transferred into the dry room for filling activities in small quantities. Care should be taken after 3 months, and the water level and HF level checked of the electrolytes to ensure that it can still be used.

6. References

1. Blomgren GE. The Development and Future of Lithium Ion Batteries. J Electrochem Soc. 2017;164(1):A5019–25.
2. Goodenough JB, Park K. The Li-Ion Rechargeable Battery : A Perspective. J Am Chem Soc. 2013;135(4):1167–76.
3. Wood III DL, Li J, Daniel C. Prospects for reducing the processing cost of lithium ion batteries. J Power Sources [Internet]. Elsevier B.V; 2015;275:234–42. Available from: http://dx.doi.org/10.1016/j.jpowsour.2014.11.019
4. Malmgren S, Ciosek K, Lindblad R, Plogmaker S, Kühn J, Rensmo H, et al. Consequences of air exposure on the lithiated graphite SEI. Electrochim Acta [Internet]. Elsevier Ltd; 2013;105:83–91. Available from: http://dx.doi.org/10.1016/j.electacta.2013.04.118
5. Li J, Daniel C, An SJ, Wood D. Evaluation Residual Moisture in Lithium-Ion Battery Electrodes and Its Effect on Electrode Performance. MRS Adv. 2016;1(15):1029–35.
6. Jung R, Morasch R, Karayaylali P, Phillips K, Maglia F, Stinner C, et al. Effect of Ambient Storage on the Degradation of Ni-Rich Positive Electrode Materials (NMC811) for Li-Ion Batteries. J Electrochem Soc. 2018;165(2):A132–41.
7. Shkrob IA, Gilbert JA, Phillips PJ, Klie R, Haasch RT, Bareno J, et al. Chemical Weathering of Layered Ni-Rich Oxide Electrode Materials : Evidence for Cation Exchange. J Electrochem Soc. 2017;164(7):A1489–98.
8. Kubota K, Komaba S. Review — Practical Issues and Future Perspective for Na-Ion Batteries. J Electrochem Soc. 2015;162(14):A2538–50.
9. Sousa RE, Kundu M, Goren A, Silva MM, Liu L, Costa CM, et al. Poly(vinylidene fluoride-co-cholorotrifluoroethylene) (PVDF-CTFE) lithium-ion battery separator membranes prepared by phase inversion. RSC Adv. 2015;5:90428–36.
10. Roberts S, Kendrick E. The re-emergence of sodium ion batteries : testing , processing , and manufacturability. Nanotechnol Sci Appl. 2018;11:23–33.
11. Biensan P, Godiveau O, Simon B. COMPOSITION FOR A POSITIVE ELECTRODE, A METHOD OF PREPARING SAID COMPOSITION, AND THE USE OF AN ORGANIC ACID COMPOUND FOR NEUTRALIZING LIOH. France: United States Patents; US5932632A, 1999.
12. Schweiger H, Multerer M, Wietelmann U, Panitz J, Burgemeister T, Gores HJ. NMR Determination of Trace Water in Lithium Salts for Battery Electrolytes. J Electrochem Soc. 2005;152(3):A622–7.
13. Lux SF, Chevalier J, Lucas IT, Kostecki R. HF Formation in LiPF 6 -Based Organic Carbonate Electrolytes. ECS Electrochem Lett. 2013;2(12):A121–3.
14. Dupin J, Gonbeau D, Vinatier P, Levasseur A. Systematic XPS studies of metal oxides , hydroxides and peroxides. Phys Chem Chem Phys. 2000;2:1319–24.
15. Daheron L, Martinez H, Dedryvere R, Baraille I, Menetrier M, Denage C, et al. Surface Properties of LiCoO 2 Investigated by XPS Analyses and Theoretical Calculations. J Phys Chem C. 2009;113:5843–52.

Table 1: The elemental composition for the 'as received' cathode and after 12 weeks in a vacuum oven at 50 °C, dry room and at 25 °C in standard atmospheric conditions as determined by XPS analysis

Storage Environment			As received		Vacuum Oven		Dry Room		Laboratory	
Element	Bonding Environment	Peak Position	Atomic %	Element %	Atomic %	Element %	Atomic %	Element %	Atomic %	Element %
Carbon (C 1s)	Graphitic C-C	284.30	17.30	50.19	13.55	58.21	16.94	46.57	20.18	42.62
	Pi-Pi*	290.87	0.87		0.88		1.1		1.32	
	sp3 (C-C, C-H)	284.80	9.03		25.83		4.82		1.06	
	C-O	285.88	10.41		9.12		14.53		9.7	
	C=O	287.84	1.83		0.81		1.31		1.26	
	C=O-OH	288.84	1.39		1.84		1.08		0.89	
	CF_2	290.37	9.36		6.18		6.79		8.21	
Oxygen (O 1s)	NiO	529.25	9.13	20.16	4.44	13.45	8.16	18.66	6.75	23.49
	$M\text{-}(OH)_x$	530.96	8.88		2.29		4.25		8.81	
	C-O-C	531.92	2.15		6.72		6.25		7.93	
Sulphur (S 2p)	$M(SO_4)$	168.74	0.34	0.51	0.44	0.66	0.35	0.52	0.29	0.43
	$M(SO_4)$	169.92	0.17		0.22		0.17		0.14	
	LiF	684.52	23.46	25.05	0.40	16.03	0.64	17.54	0.31	16.58
	AlF_3	687.62	1.59		15.63		16.9		16.27	
Manganese (Mn 3p)	MnO_2	49.36	0.46	0.60	0.61	0.70	0.93	1.11	0.98	1.17
	MnO_2	51.33	0.14		0.09		0.18		0.19	
Lithium (Li 1s)	$LiNiO_2$	54.08	0.25	0.25	6.99	6.99	9.83	9.83	10.25	10.25
Cobalt (Co 3p)	CoO	60.87	0.64	0.64	0.59	0.59	0.93	0.93	0.92	0.92
Nickel (Ni 3p)	NiO	67.17	0.70	2.17	0.4	1.43	0.51	1.98	0.71	2.12
	NiO	69.17	1.47		1.03		1.47		1.41	
Aluminium (Al 2p)	$(Al_2O_3.xH_2O)$ / $Al(OH)_3$	74.00	0.43	0.43	1.93	1.93	2.85	2.85	2.44	2.44

Table 2: The elemental composition for the 'as received' anode and after 12 weeks in a vacuum oven at 50 °C, dry room and at 25 °C in standard atmospheric conditions as determined by XPS analysis

Storage Environment			As received		Vacuum Oven		Dry Room		Laboratory	
Element	Bonding Environment	Peak Position	Atomic %	Element %	Atomic %	Element %	Atomic %	Element %	Atomic %	Element %
Carbon (C 1s)	Graphitic C-C	284.3	29.95	80.01	16.13	84.50	25.51	79.94	36.30	79.34
	Pi-Pi*	291.06	27.22		1.05		1.28		2.37	
	sp3 (C-C, C-H)	284.80	4.09		36.81		30.28		21.06	
	C-O	285.93	9.97		13.97		8.75		4.69	
	C=O	286.88	4.56		6.33		10.22		11.00	
	O=C-OH	288.45	2.32		1.85		3.36		3.78	
	(C=O)-O-R	287.85	-		3.18		-		-	
	CO_3	289.87			1.09					
Oxygen (O 1s)	C-O-C	531.65	3.55	15.54	3.16	14.41	4.48	15.46	4.71	15.85
	O-C-O	533.21	11.62		10.55		10.88		11.11	
Sodium (Na 1s)	Na 1s	1071.99	4.35	4.35	1.04	1.04	4.57	4.57	4.80	4.80

Table 3: Averaged electrochemical data for cells manufactured using electrodes stored in a) a vacuum oven, b) a dry room and c) a temperature controlled laboratory at regular intervals over a 5-month period

Storage length		2 weeks	4 weeks	8 weeks	12 weeks	16 weeks	20 weeks
Vacuum oven	Electrode weight (g)	0.0448	0.0448	0.047	0.0448	0.0448	0.0447
	Formation capacity (mA h)	6.21	6.16	6.22	6.28	6.19	6.43
	Formation Loss (%)	12.19	11.53	14.90	14.65	13.10	16.59
	V drop after formation (V)	0.017	0.017	0.022	0.021	0.016	0.116
	V drop during ageing (V)	0.065	0.052	0.066	0.08	0.052	0.042
	2nd discharge (mA h)	5.453	5.45	5.293	5.36	5.379	5.363
Dry room	Electrode weight (g)	0.04484	0.0446	0.0448	0.04466	0.04455	0.0447
	Formation capacity (mA h)	6.19	6.09	6.18	6.2	6.12	6.01
	Formation Loss (%)	12.44	10.97	12.10	14.18	12.25	12.03
	V drop after formation (V)	0.016	0.016	0.016	0.019	0.018	0.035
	V drop during ageing (V)	0.065	0.079	0.067	0.063	0.057	0.053
	2nd discharge (mA h)	5.42	5.422	5.432	5.321	5.37	5.287
Laboratory	Electrode weight (g)	0.04514	0.0449	0.0451	0.04481	0.04521	0.04503
	Formation capacity (mA h)	6.15	6.12	6.08	6.08	6.06	5.99
	Formation Loss (%)	11.02	10.75	16.27	12.68	10.26	10.90
	V drop after formation (V)	0.018	0.019	0.021	0.024	0.026	0.029
	V drop during ageing (V)	0.061	0.059	0.062	0.073	0.069	0.058
	2nd discharge (mA h)	5.472	5.462	5.091	5.309	5.438	5.337

Table 4: Resistance contributed by the SEI layer extracted from the EIS data shown in figures 9 &10 showing how the samples manufactured using 5-month stored electrodes show a dramatic increase in impedance with cycling

Age of cell	Fresh electrodes (Ω)	Stored electrodes (Ω)
After formation	3.17	4.65
After 50 cycles	3.53	6.30
After 100 cycles	3.59	20.62
After 200 cycles	3.74	35.0
After 500 cycles	5.42	51.27

Additional Information

Funding Statement

Funding was through HEDB: High Energy Density Battery, an advanced propulsion centre funded project, and the WMG HMV Catapult.

Competing Interests
The authors have no competing interests

Authors' Contributions
S Gorman and T Pathan have; 1) substantial contributed to conception and design, or acquisition of data, or analysis and interpretation of data and 2) drafted the article. E Kendrick has 2) drafted the article and revised it critically for important intellectual content; and given 3) final approval of the version to be published.